ARTHRITIS & RHEUMATISM
Vol. 65, No. 3, March 2013, pp 681–692
DOI 10.1002/art.37800

Host-Derived CD4+ T Cells Attenuate Stem Cell–Mediated Transfer of Autoimmune Arthritis in Lethally Irradiated C57BL/6.g7 Mice

Narendiran Rajasekaran, Nan Wang, Phi Truong, Cornelia Rinderknecht, Claudia Macaubas, Georg F. Beilhack, Judith A. Shizuru, and Elizabeth D. Mellins

Objective. **In the K/BxN mouse model of inflammatory arthritis, T cells carrying a transgenic T cell receptor initiate disease by helping B cells to produce arthritogenic anti–glucose-6-phosphate isomerase (anti-GPI) autoantibodies. We found that lethally-irradiated lymphocyte-deficient C57BL/6 (B6).g7 (I-A^{g7}+) recombinase-activating gene–deficient (Rag$^{-/-}$) mice reconstituted with K/BxN hematopoietic stem and progenitor cells exhibit arthritis by week 4. In contrast, healthy B6.g7 recipients of K/BxN hematopoietic stem and progenitor cells show only mild arthritis, with limited extent and duration. The objective of this study was to investigate the factors responsible for the attenuation of arthritis in B6.g7 recipients.**

Methods. **Antibody responses were measured by enzyme-linked immunosorbent assay. Fluorescence-activated cell sorting analyses were performed for testing chimerism, expression of markers of activation and suppression, tetramer binding, and intracellular cytokines in CD4+ T cells. Suppressive activity of CD4+ T cells was studied by adoptive transfer.**

Results. **Titers of anti-GPI antibodies in reconstituted B6.g7 mice were ~60-fold lower than in reconstituted B6.g7 Rag$^{-/-}$ mice. Examination of chimerism in the reconstituted B6.g7 mice showed that B cells and myeloid cells in these mice were donor derived, but CD4+ T cells were primarily host derived and enriched for cells expressing the conventional regulatory markers CD25 and FoxP3. Notably, CD4+CD25−FoxP3− T cells expressed markers of suppressive function (CD73 and folate receptor 4), and delayed disease after adoptive transfer. Activation of donor-derived CD4+ T cells was reduced, and thymic deletion of these cells appeared increased.**

Conclusion. **Despite myeloablation, host CD4+ T cells having a regulatory phenotype emerge in these mice and attenuate autoimmunity.**

Autoimmune diseases occur when tolerance to self antigen fails and the immune system initiates attack against self tissues. Rheumatoid arthritis (RA) is an autoimmune disease in which T cells have been proposed to recognize autoantigen and participate in effector pathways (1,2). Initial bone marrow transplant experiments in mice demonstrated that the ability to transfer autoimmune arthritis rests within the hematopoietic compartment (3). These findings led to the idea of using bone marrow transplantation as therapy for RA (4). Autologous hematopoietic stem cell transplantation (HSCT) has been tried as treatment for severe autoimmune diseases in humans (4). However, fatal infections due to insufficient recovery of T cells and relapses

Supported by grants from the Arthritis Foundation (to Dr. Rajasekaran), the Juvenile Diabetes Research Foundation (to Dr. Wang), the NIH (grant DK-067559 to Drs. Beilhack and Shizuru and grants AI-075253 and DK-079163 to Dr. Mellins), the H. L. Snyder Medical Foundation (Fellowship Award to Dr. Shizuru), the Stinehart/Reed Foundation (Diabetes Research Award to Dr. Shizuru), the Rheumatology Research Foundation of the American College of Rheumatology (to Dr. Mellins), the Juvenile Diabetes Research Foundation (to Dr. Mellins), and in part by the Stanford University NIH/National Center for Research Resources Clinical and Translational Science Award (UL1-RR-025744) and the Lucile Packard Foundation for Children's Health.

Narendiran Rajasekaran, PhD, Nan Wang, PhD, Phi Truong, BS, Cornelia Rinderknecht, PhD (current address: Genentech, Inc., South San Francisco, California), Claudia Macaubas, PhD, Georg F. Beilhack, MD (current address: Medical University of Vienna, Vienna, Austria), Judith A. Shizuru, MD, PhD, Elizabeth D. Mellins, MD: Stanford University School of Medicine, Stanford, California.

Dr. Macaubas has received consulting fees, speaking fees, and/or honoraria from Novartis (less than $10,000). Dr. Mellins has received consulting fees, speaking fees, and/or honoraria from Novartis and Genentech (less than $10,000 each).

Address correspondence to Elizabeth D. Mellins, MD, CCSR 2105c, Stanford University School of Medicine, 300 Pasteur Drive, Stanford, CA 94305-5164. E-mail: mellins@stanford.edu.

Submitted for publication July 9, 2012; accepted in revised form November 15, 2012.

of autoimmunity likely due to the persistence of autoreactive clones have limited the use of this approach (5).

Studies in C57BL/6 (B6) mice demonstrated that following lethal irradiation and transplantation of bone marrow (BM), the myeloid leukocytes were almost completely donor derived, but significant numbers (25%) of CD4+ T cells were recipient derived (6). In another study, although host-derived cells were the major constituent (60–80%) of the Treg cell compartment 5 weeks following autologous BM transplantation (7), donor-derived Treg cells were detectable ~2–3 weeks posttransplant and became the major source of Treg cells by 8 weeks posttransplant. The initial predominance of the host-derived Treg cells in these mice was due to their proliferative expansion during the first 5 weeks posttransplant. The presence of host-derived Treg cell–enriched CD4+ T cells in these studies has raised the hope of devising a cell-based strategy to inhibit relapse of autoimmunity in human HSCT. However, more detailed information on the emergence and function of these host-derived Treg cells is needed.

Here, we describe experiments with a novel HSCT-based model of autoimmune disease. We used stem cells from the spontaneous K/BxN model of autoimmune arthritis in which class II–restricted, transgenic T cell receptors (TCRs) drive disease. K/BxN mice are a cross of KRN mice with the NOD strain; KRN mice carry a transgenic TCR that recognizes a glucose-6-phosphate isomerase (GPI) peptide bound to the NOD class II molecule I-A^{g7} of the major histocompatibility complex (MHC). (KRN × NOD)F1 mice show severe distal joint inflammation, with onset at age ~4–5 weeks. The severe symmetric polyarthritis in these mice is dependent on expression of the KRN TCR (8) and T cell help for B cells that make pathogenic anti-GPI antibodies (9). The anti-GPI antibodies form immune complexes with GPI, triggering a joint-specific inflammatory response mediated by neutrophils, macrophages, natural killer cells, and Th17 cells (9,10). In the K/BxN model, CD25+FoxP3+ Treg cells are selected in the thymus and enriched in the spleen (~20%) and draining lymph nodes (LNs) during arthritis. The Treg cells mediate suppressive function in vitro but do not inhibit severe arthritis in the mice (11). However, Treg cell depletion in K/BxN mice results in multiorgan inflammation with persistent arthritis (12).

The crucial role of I-A^{g7} in the K/BxN arthritis model was shown by breeding experiments: B6 or BALB/c mice carrying the I-A^{g7} gene, when crossed into B6 mice carrying the KRN TCR, yield offspring that develop arthritis similar to that in K/BxN mice (13). We predicted that transfer of hematopoietic stem and progenitor cells from K/BxN mice into myeloablated B6.g7 mice (I-A^{g7} expression on B6 background) would result in autoimmune arthritis; surprisingly, however, autoimmunity in recipient mice was highly attenuated. Here, we identify immunosuppressive roles for host-derived CD4+ T cells with regulatory phenotypes, including CD25−FoxP3−CD73+ cells.

MATERIALS AND METHODS

Mice. NOD mice and B6.g7 mice derived from B6 mice expressing the NOD class II MHC molecule I-A^{g7} were obtained from The Jackson Laboratory. Recombinase-activating gene (Rag)–deficient B6.g7 (B6.g7 $Rag^{-/-}$) mice lack T and B cells (Beilhack GF, Shizuru JA: unpublished observations). KRN mice with a transgenic TCR against GPI were kindly provided by Dr. Diane Mathis (Harvard Medical School, Boston, MA). The arthritic K/BxN mice were obtained by crossing KRN mice with NOD mice, as is standard. All animals were bred, housed, and cared for in the Stanford Veterinary Service Center under the approval of the Administrative Panel for Laboratory Animal Care, protocol no. 15867.

Hematopoietic stem and progenitor cell isolation. Hematopoietic stem and progenitor cells were isolated as described, with some modifications (14). BM cells were harvested and selected for c-Kit+ cells using the MACS system (Miltenyi Biotec). The c-Kit+ BM cells were then sorted in a FACSAria cell sorter (BD Biosciences) for c-Kit+Sca-1^{high}Lin− cells after staining with antibodies (further information is available at http://med.stanford.edu/genetherapy/research/related_sites.html). All antibodies were obtained from eBioscience. Fluorescence-activated cell sorting (FACS) was performed at the Stanford Shared FACS Facility at Stanford University.

HSCT. Recipient mice (B6.g7 or B6.g7 $Rag^{-/-}$) ages 3–4 months were lethally irradiated with a Phillips Unit irradiator (250 kV, 15 mA) at 980 rads (in 2 doses with a 4-hour interval). Irradiated mice were reconstituted with hematopoietic stem and progenitor cells from 3–5-month-old donors (K/BxN mice) 3 hours after irradiation. Hematopoietic stem and progenitor cells (10,000–12,000) in 200 μl phosphate buffered saline (PBS) were given to each recipient by tail vein injection. The reconstituted mice were maintained on trimethoprim/sulfamethoxazole (suspension; Hi-Tech Pharmacal) in drinking water up to 3 months posttransplant. Control mice that received irradiation only (without transplantation) died within 2 weeks.

Antibody and tetramer staining and flow cytometry analyses. Thymus, spleen, and popliteal LNs were harvested from mice. Surface staining was done with various antibodies directly conjugated to fluorochromes (further information is available at http://med.stanford.edu/genetherapy/research/related_sites.html). For biotin-labeled antibodies, Pacific Orange–conjugated streptavidin (Invitrogen) was added and incubated for an additional 30 minutes. For intracellular FoxP3 staining, cells were treated with fixation/permeabilization reagent (eBioscience) followed by staining with antibodies (eBioscience). For cytokine stimulation and intracellular staining, spleen cells were suspended in complete Iscove's modified Dulbecco's

medium (10% fetal bovine serum, 1% L-glutamine, 0.1% β-mercaptoethanol) and incubated for 4 hours at 37°C with or without Leukocyte Activation Cocktail (BD Biosciences). Cell viability was assessed by staining with Live Dead Aqua (Invitrogen). Subsequently, cells were permeabilized and stained with fluorescein isothiocyanate–conjugated anti–interleukin-17 (anti–IL-17) antibody (TC11-18H10), phycoerythrin (PE)–conjugated anti–interferon-γ (anti-IFNγ) antibody (XMG1.2), and allophycocyanin-conjugated anti-FoxP3 antibody (FJK-16s).

For tetramer staining, the single-cell suspension was blocked with 0.5 mg/ml Fc block for 10 minutes on ice. Cells were then washed and stained with PE-labeled MHC/GPI peptide tetramer (kindly provided by Dr. Luc Teyton, The Scripps Research Institute, La Jolla, CA) at a final concentration of 10 μg/ml for 1 hour at room temperature (15). PE-labeled MHC/hen egg lysozyme peptide tetramer was used as negative control in all experiments. Costaining of surface markers was done as mentioned above. In all antibody staining experiments, data were collected on an LSRII flow cytometer (BD Biosciences) and analyzed with FlowJo software (Tree Star), gating on single cell populations. All FACS analyses were performed at the Stanford Shared FACS Facility at Stanford University.

Evaluation of autoimmune disease. Mice were assessed by clinical arthritis index and circulating anti-GPI antibody titer. The clinical arthritis index was tallied from the degree of inflammation of each ankle, based on redness and swelling measured with a pocket thickness gauge (Mitutoyo). Scores were as follows: 0 = none; 0.25 = mild; 0.5 = moderate; 1 = severe, with 4 being the maximum score in mice with full-blown arthritis (16). The mean ± SEM score per animal group was calculated. GPI titer was determined by enzyme-linked immunosorbent assay (ELISA). Specifically, ELISA plates were coated with GPI protein (1–4 μg) and blocked with PBS containing 0.05% Tween 20 and 1% fat-free powdered milk followed by addition of diluted serum at 100 μl/well. After incubation at 37°C for 2 hours, the plates were washed and incubated with horseradish peroxidase–conjugated goat anti-mouse IgG antibody (1:5,000 dilution; Millipore) for 1 hour before adding tetramethylbenzidine substrate (BD OptEIA kit; BD Biosciences). Results were read out with a SpectraMax 190 Absorbance Microplate Reader (Molecular Devices) after stopping the reaction with 50 μl H_2SO_4 (1*M* stock). For joint histopathology, ankle joints were fixed in 4% phosphate buffered formaldehyde and then sectioned and stained with hematoxylin and eosin by Premier Laboratory. Microscopy was performed with an Axioplan 2 instrument (Carl Zeiss Microscopy).

Adoptive transfer. Spleen cells and LN cells were harvested from K/BxN→B6.g7 mice 3 months after reconstitution of hematopoietic stem and progenitor cells. Cells were resuspended in Hanks' balanced salt solution buffer with 2% fetal calf serum and surface stained with antibodies against CD45.2, CD45.1, CD4, CD25, folate receptor 4 (FR4), and CD73 to identify host- and donor-derived regulatory cells. Host-derived CD4+CD25^{high} cells and CD4+CD25−CD73+

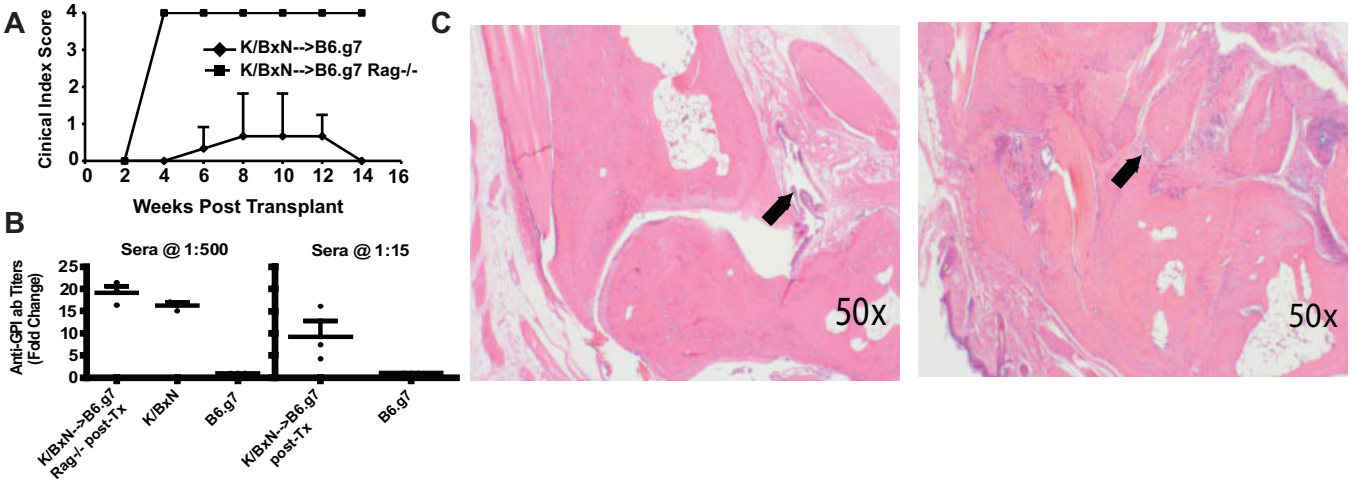

Figure 1. Transfer of hematopoietic stem and progenitor cells from K/BxN donors into immunocompetent C57BL/6 (B6).g7 recipients results in protection against autoimmunity. **A,** Hematopoietic stem and progenitor cells isolated from K/BxN mouse bone marrow were transferred into lethally irradiated B6.g7 and B6.g7 recombinase-activating gene–deficient ($Rag^{-/-}$) recipients. Onset and progression of arthritis were measured using a clinical arthritis index (see Materials and Methods). Values are the mean ± SEM (n = 3 mice). **B,** Lethally irradiated B6.g7 $Rag^{-/-}$ or B6.g7 mice were reconstituted with K/BxN-derived hematopoietic stem and progenitor cells. Mice were bled for sera 10 weeks posttransplant (post-Tx), and titers of anti–glucose-6-phosphate isomerase (anti-GPI) autoantibodies (Ab) were measured by enzyme-linked immunosorbent assay. Sera from K/BxN and B6.g7 $Rag^{-/-}$ recipients were diluted (left), and sera from B6.g7 recipients were diluted (right). Antibody titers were normalized with the levels in B6.g7 mice, set to 1. Values are the mean ± SEM (n = 3 mice). **C,** Shown is hematoxylin and eosin staining of ankle sections from lethally irradiated B6.g7 mice (left) and B6.g7 $Rag^{-/-}$ mice (right) that were reconstituted with K/BxN hematopoietic stem and progenitor cells and killed 12 weeks posttransfer. A mild synovial proliferation is seen in the reconstituted B6.g7 mouse (**arrow**). Severe bone and cartilage destruction is observed in the reconstituted B6.g7 $Rag^{-/-}$ mouse (**arrow**). Results are representative of 3 independent experiments in **A** and **B** and 2 independent experiments in **C**.

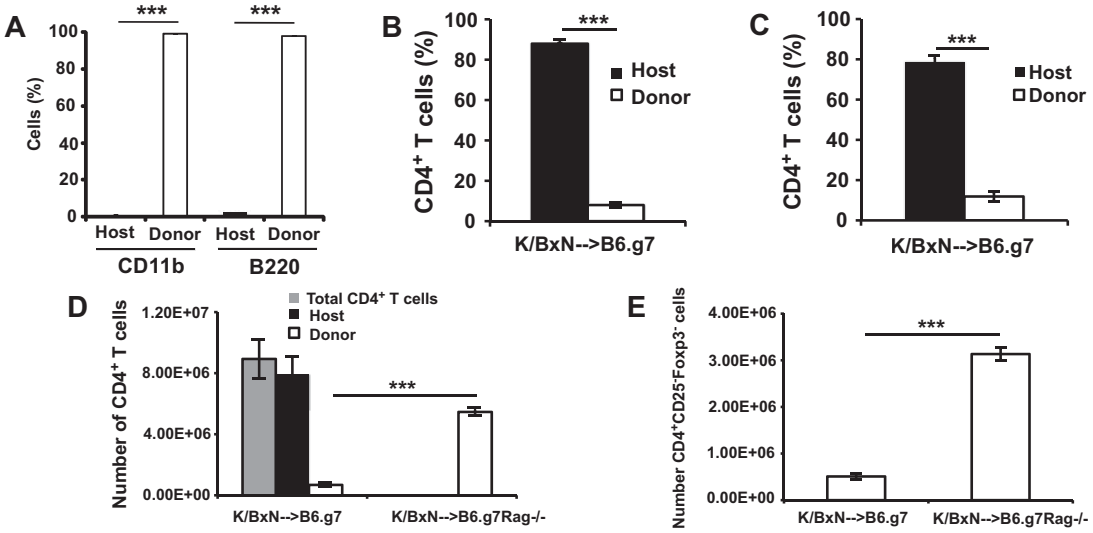

Figure 2. Emergence of host-derived CD4+ T cells in reconstituted B6.g7 mice. **A,** Results of flow cytometric analysis of spleen cells from K/BxN→B6.g7 mice killed 12 weeks posttransplant. Cells were stained for CD11b (myeloid cells) and B220 (B cells) and analyzed to determine host (CD45.2+) or donor (CD45.1+) origin. Values are the mean from 3 animals. *** = $P < 0.0001$ by *t*-test. **B,** Frequency of host- and donor-derived splenic CD4+ T cells. **C,** Frequency of host- and donor-derived CD4+ T cells in the draining lymph node. **D,** Absolute numbers of host- and donor-derived splenic CD4+ T cells in K/BxN→B6.g7 mice as well as absolute numbers of donor-derived splenic CD4+ T cells in K/BxN→B6.g7 $Rag^{-/-}$ mice. Absolute numbers were determined by multiplying the total number of cells in each spleen (determined using a Coulter counter) by the percentage of the host- and donor-derived CD4+ T cells. **E,** Absolute number of CD4+CD25−FoxP3− T cells in K/BxN→B6.g7 $Rag^{-/-}$ mice in comparison to the donor-derived CD4+CD25−FoxP3− T cells in K/BxN→B6.g7 chimeras. Values in **B–E** are the mean ± SEM from 6 animals. *** = $P < 0.001$ by *t*-test. Data are representative of 3 independent experiments in **A–C** or 2 independent experiments in **D** and **E**. See Figure 1 for definitions.

FR4+ cells were sorted using a FACSAria cell sorter and injected separately (5×10^5 cells per mouse) into B6.g7 $Rag^{-/-}$ recipients that had been reconstituted with K/BxN hematopoietic stem and progenitor cells 20 days earlier. Mice were then monitored for onset and progression of arthritis as above.

Statistical analysis. The groups were compared using Student's unpaired 2-tailed *t*-test. GraphPad Prism software, version 5 was used for statistical analysis.

RESULTS

B6.g7 mice reconstituted with hematopoietic stem and progenitor cells from K/BxN mice have mild, transient disease. In an effort to create an HSCT model for autoimmune arthritis, lethally irradiated B6.g7 $Rag^{-/-}$ mice were reconstituted with hematopoietic stem and progenitor cells (c-Kit+Sca-1^{high}Lin−) isolated from K/BxN mice. The recipients were followed up for development of arthritis. All developed severe arthritis (Figure 1A) and had high-titer anti-GPI autoantibodies (Figure 1B) comparable to those in transgenic K/BxN mice. In contrast, lethally irradiated B6.g7 mice reconstituted with hematopoietic stem and progenitor cells from K/BxN mice developed very mild arthritis that disappeared by week 14 (Figure 1A) and had very low-titer, circulating anti-GPI autoantibodies (Figure 1B). Joint histopathology showed minimal inflammatory cell infiltrates in the K/BxN→B6.g7 mice, whereas the K/BxN→B6.g7 $Rag^{-/-}$ chimeras showed prominent cell infiltration and severe bone destruction (Figure 1C). Thus, transfer of K/BxN hematopoietic stem and progenitor cells into immunocompetent B6.g7 mice resulted in attenuated autoimmunity compared to transfer into immunodeficient B6.g7 $Rag^{-/-}$ mice.

Reduced donor-derived CD4+ T cells in reconstituted B6.g7 mice compared to reconstituted B6.g7 $Rag^{-/-}$ mice. In the K/BxN mouse, CD4+ T cells bearing the KRN TCR and antigen-presenting cells expressing the class II MHC molecule I-A^{g7} are required for the initiation and progression of autoimmunity. To determine if disease resistance in the B6.g7 mice was due to incomplete reconstitution of T or B cells, we analyzed splenocytes from B6.g7 recipients 12 weeks after transplant of hematopoietic stem and progenitor cells. Compared to K/BxN mice, the K/BxN→B6.g7 chimeras showed comparable ratios of CD4+:CD8+ T cells, and comparable proportions of B220+ B cells, with a lower

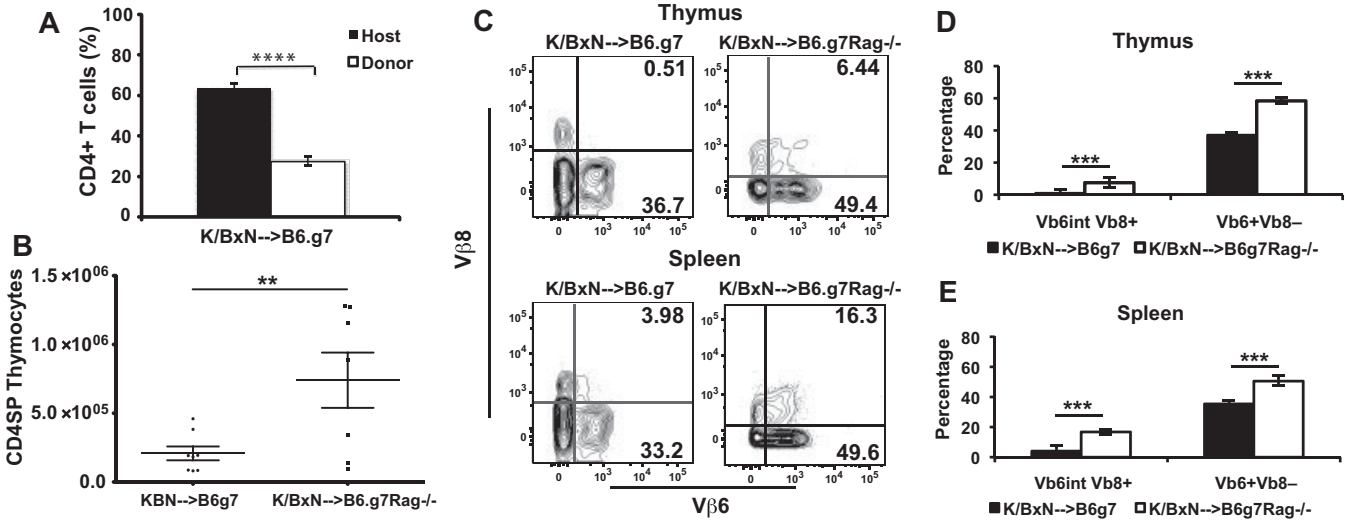

Figure 3. Host-derived CD4+ single-positive (CD4SP) T cells are predominant in the thymus. **A,** Frequency of host- and donor-derived CD4+ T cells in the thymus. Thymocytes from K/BxN→B6.g7 mice killed 12 weeks posttransplant were stained for CD4 and CD45.2 (host) or CD45.1 (donor). **B,** Absolute numbers of host- and donor-derived thymic CD4+ single-positive T cells, determined by multiplying the total number of cells in each thymus (determined using a Coulter counter) by the percentage of the host- and donor-derived CD4+ T cells. Bars in **A** and **B** show the mean ± SEM from 8 K/BxN→B6.g7 mice and from 7 K/BxN→B6.g7 Rag$^{-/-}$ mice. Dots in **B** represent individual mice ** = $P < 0.001$; **** = $P < 0.0002$ by *t*-test. Data are representative of 2 independent experiments. **C**, Expression of T cell receptor β chains $V_\beta6$ and $V_\beta8$ on donor-derived CD4+ T cells. Flow cytometry plots show the frequency of $V_\beta6$- and $V_\beta8$-expressing cells in donor-derived CD4+CD25−FoxP3− cells in the thymus and spleen in K/BxN→B6.g7 mice and K/BxN→B6.g7 Rag$^{-/-}$ mice killed 12 weeks posttransplant. **D** and **E,** Frequency of $V_\beta6^{intermediate}V_\beta8$+ and $V_\beta6$+$V_\beta8$− populations in the thymus (**D**) and spleen (**E**) of K/BxN→B6.g7 mice and K/BxN→B6.g7 Rag$^{-/-}$ mice. Values are the mean ± SEM from 6 K/BxN→B6.g7 mice and from 4 K/BxN→B6.g7 Rag$^{-/-}$ mice. *** = $P < 0.0004$ by *t*-test. KBN = K/BxN (see Figure 1 for other definitions).

proportion of CD11b+ cells (neutrophils), presumably reflecting the reduced inflammatory response in these mice (further information is available at http://med.stanford.edu/genetherapy/research/related_sites.html). However, compared to B6.g7 mice, the proportion of CD4+ T cells was low in both the chimera and K/BxN mice, likely due to negative selection of the self-reactive transgenic TCR (13).

To distinguish the host and donor hematopoietic cells in the chimera, we used the congenic markers CD45.1 and CD45.2 (further information is available at http://med.stanford.edu/genetherapy/research/related_sites.html). Approximately 98% of B cells and neutrophils were of donor origin (Figure 2A), but only ~10% of splenic CD4+ T cells were of donor origin (Figure 2B). As pathogenic autoreactive CD4+ T cells undergo expansion in the draining LNs of the inflamed target organs in the K/BxN mice (13), we assessed chimerism in draining LNs. The joint-draining popliteal LNs of the K/BxN→B6.g7 chimera showed percentages of donor-derived CD4+ T cells comparable to those in spleen (Figure 2C). The absolute numbers of donor-derived splenic CD4+ T cells (Figure 2D) and CD4+CD25− FoxP3− T cells (Figure 2E) were also reduced in the B6.g7 recipients compared to the B6.g7 Rag$^{-/-}$ recipients. Thus, insufficient numbers of KRN TCR+, donor-derived CD4+ Teff cells is one possible explanation for attenuated autoimmunity in K/BxN→B6.g7 chimeras. However, the appearance of autoantibodies and joint infiltrates in the K/BxN→B6.g7 chimeras indicates that Teff cell numbers were sufficient to break tolerance.

K/BxN→B6.g7 chimeras have reduced proportions of transgenic TCR+ or I-A^{g7}/GPI tetramer+ donor-derived CD4+ T cells. We next analyzed the thymi of the K/BxN→B6.g7 chimeras and found that the majority of CD4+ single-positive T cells were host derived and absolute numbers of donor-derived CD4+ single-positive T cells were reduced compared to thymocytes in the K/BxN→B6.g7 Rag$^{-/-}$ chimeras (Figures 3A and B). The β-chain of the KRN TCR in the K/BxN mice is $V_\beta6$ (13). Selection of KRN TCR–expressing CD4+ single-positive T cells can be evaluated by the expression of $V_\beta6$ compared to the expression of other variable regions from endogenous TCR loci, like $V_\beta8$. In the thymus and spleen of the K/BxN→B6.g7 Rag$^{-/-}$ mice, we found that ~50% of the CD4+ T cells were

$V_\beta 6+V_\beta 8-$ and ~15% of T cells were $V_\beta 6^{intermediate}V_\beta 8+$ (Figures 3C–E), an expression pattern similar to that in K/BxN mice (13). K/BxN→B6.g7 mice showed substantially lower proportions of each subset, including among CD4+ single-positive thymocytes (Figures 3C–E). To enumerate circulating cells expressing the KRN TCR based on their recognition of I-A^{g7} molecules with bound $GPI^{282–294}$ peptide (17), we used I-A^{g7}/$GPI^{282–294}$ peptide tetramers to stain CD4+ T cells in the blood obtained from K/BxN→B6.g7 and K/BxN→B6.g7 $Rag^{-/-}$ mice. The frequency of donor-derived, CD4+ CD25−$V_\beta 6$+tetramer+ cells was significantly lower in the K/BxN→B6.g7 mice compared to the K/BxN→B6.g7 $Rag^{-/-}$ mice (mean ± SEM 2.53 ± 0.6% versus 12.26 ± 1.3%; $P = 0.0006$) (Figure 4A).

Donor-derived CD4+CD25−FoxP3− cells in K/BxN→B6.g7 mice are less activated than those in K/BxN→B6.g7 $Rag^{-/-}$ mice. The peripheral CD4+ T cell compartment in K/BxN mice is activated, as evidenced by expression of the activation/memory marker CD44 (18). In the arthritic K/BxN→B6.g7 $Rag^{-/-}$ chimeras, similar to the K/BxN mice, a high proportion of the donor-derived CD4+CD25−FoxP3− cells were $CD44^{high}$ (mean ± SEM 62.5 ± 3.1%). In contrast, significantly fewer donor-derived CD4+CD25−FoxP3− cells in the K/BxN→B6.g7 chimeras were $CD44^{high}$ (mean ± SEM 28.7 ± 2.8%) ($P < 0.0001$) (Figure 4B). To further characterize the activation state of donor-derived CD4+ T cells, we measured their expression of the inflammatory cytokines IFNγ and IL-17 after stimulation with phorbol myristate acetate (Figures 4C and D). These cytokines are known to promote arthritis in K/BxN mice (10). A higher proportion of donor-derived splenic CD4+ T cells expressed IFNγ and IL-17 in K/BxN→B6.g7 $Rag^{-/-}$ mice than in K/BxN→B6.g7 mice (for IFNγ, 21.5 ± 6.8% versus 4.19 ± 1.5%; $P < 0.0002$) (for IL-17, 2.28 ± 0.17% versus 0.36 ± 0.37%; $P < 0.013$). Taken together, these data indicate reduced activation of potentially arthritogenic T cells in the K/BxN→B6.g7 chimeras.

Host-derived CD4+ T cells are enriched for CD25+FoxP3+ Treg cells. The presence of host-derived CD4+ T cells in the spleen and thymus of K/BxN→B6.g7 chimeras indicates a possible role of these cells in attenuating autoimmunity. To investigate whether these cells had regulatory properties, we assessed levels of CD4+CD25+FoxP3+ Treg cells in the host and donor-derived CD4+ T cells in the K/BxN→B6.g7 reconsti-

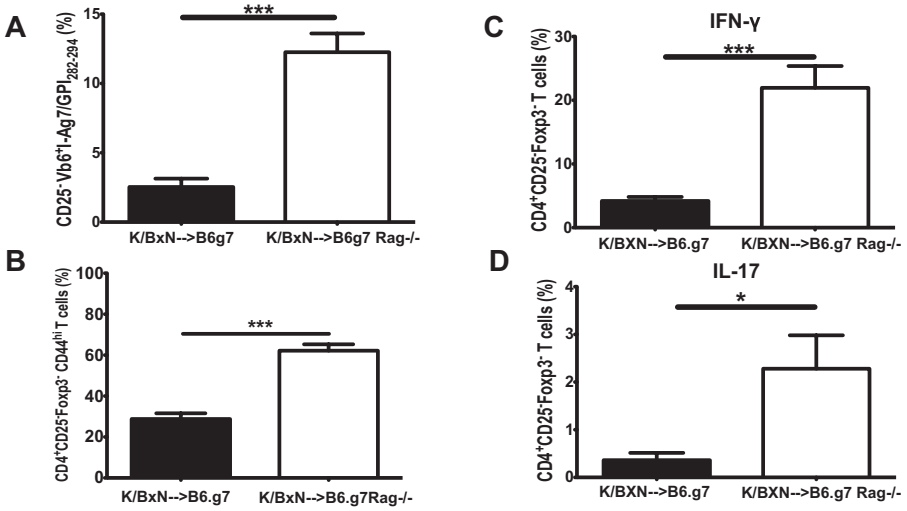

Figure 4. Presence of donor-derived CD4+ T cells with decreased activation, reduced cytokine expression, and reduced fraction of major histocompatibility complex/$GPI^{282–294}$ peptide tetramer–positive cells in K/BxN→B6.g7 mice. **A,** Frequency of donor-derived CD4+CD25−$V_\beta 6$+tetramer+ cells, determined by fluorescence-activated cell sorting staining of blood cells with I-A^{g7}/$GPI^{282–294}$ tetramer. Values are the mean ± SEM from 3 K/BxN→B6.g7 $Rag^{-/-}$ mice and 4 K/BxN→B6.g7 mice. *** = $P = 0.0006$ by unpaired 2-tailed *t*-test. Data are representative of 2 independent experiments. **B,** CD44 expression on host- and donor-derived CD4+CD25−FoxP3− cells in the spleens of K/BxN→B6.g7 chimeric mice killed 12 weeks after reconstitution. Values are the mean ± SEM from 6 K/BxN→B6.g7 $Rag^{-/-}$ mice and 4 K/BxN→B6.g7 mice. *** = $P < 0.0001$ by unpaired 2-tailed *t*-test. Data are representative of 3 independent experiments. **C,** Frequency of interferon-γ (IFNγ)–expressing cells in donor-derived CD4+CD25−FoxP3− cells in K/BxN→B6.g7 and K/BxN→B6.g7 $Rag^{-/-}$ chimeras. **D,** Frequency of interleukin-17 (IL-17)–expressing cells in donor-derived CD4+CD25−FoxP3− cells in K/BxN→B6.g7 and K/BxN→B6.g7 $Rag^{-/-}$ chimeras. We evaluated splenocytes from 6 K/BxN→B6.g7 mice and 4 K/BxN→B6.g7 $Rag^{-/-}$ mice killed 12 weeks posttransplant. Values in **C** and **D** are the mean ± SEM. * = $P < 0.013$; *** = $P < 0.0002$ by *t*-test. Data are representative of 3 independent experiments. See Figure 1 for other definitions.

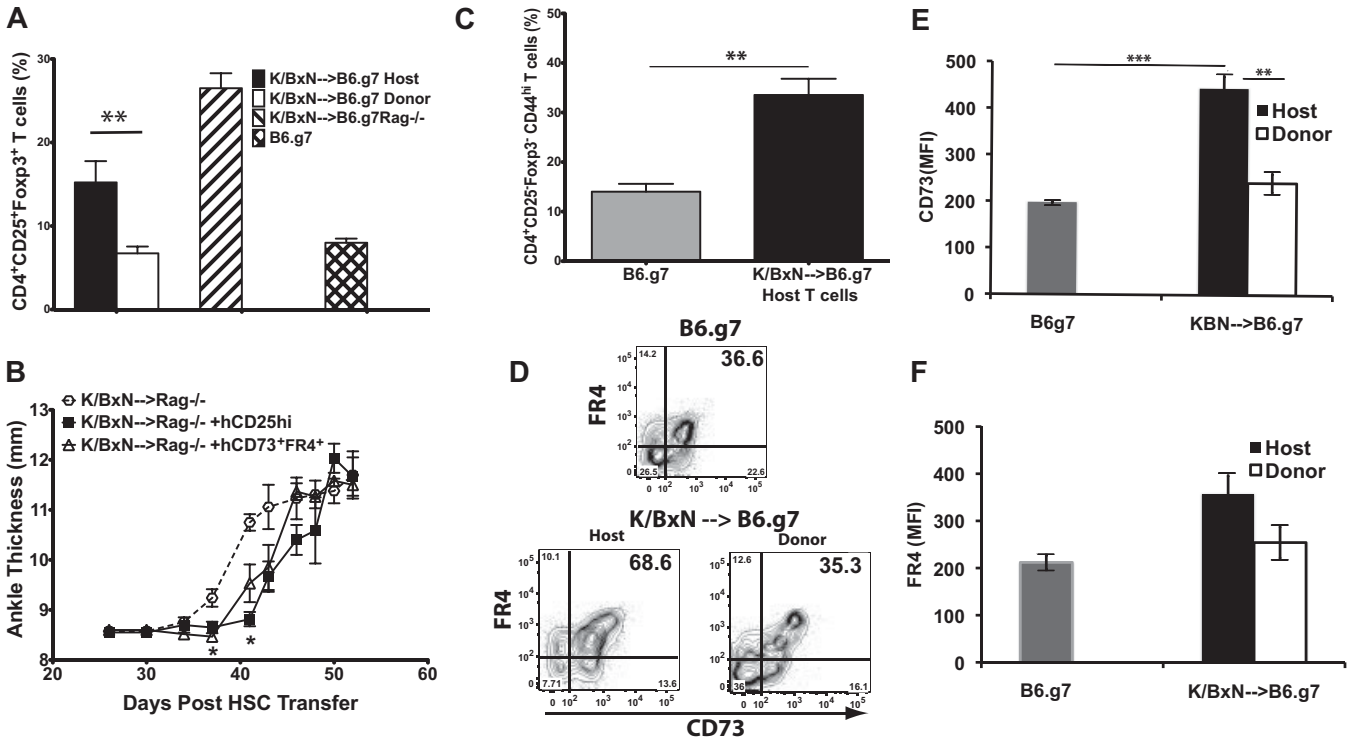

Figure 5. FoxP3 expression in CD4+CD25+ T cells in reconstituted mice and memory-like phenotype (CD44+) in host-derived CD4+CD25−FoxP3− cells. **A,** Frequency of CD4+CD25+FoxP3+ cells in the host- and donor-derived splenocytes of K/BxN→B6.g7 chimeras killed 12 weeks posttransplant. Shown also are the frequency of CD4+CD25+FoxP3+ cells in donor-derived splenocytes of K/BxN→B6.g7 $Rag^{-/-}$ mice and the frequency of CD4+CD25+FoxP3+ cells in splenocytes of B6.g7 mice. Values are the mean ± SEM (n = 9 mice) using combined data from 2 experiments. ** = $P < 0.0059$ by *t*-test. **B,** Adoptive transfer of regulatory cells as described in Materials and Methods. Development of arthritis, represented by ankle thickness, is shown until 52 days after transfer of hematopoietic stem and progenitor cells (HSC). Statistical analysis compared the ankle thickness of K/BxN→B6.g7 $Rag^{-/-}$ mice (n = 4 per group) with that of K/BxN→B6.g7 $Rag^{-/-}$ mice transferred with host-derived CD25−CD73+folate receptor 4–positive (FR4+) cells (n = 3 per group) (* = $P < 0.01$ by *t*-test on day 37) or with that of K/BxN→B6.g7 $Rag^{-/-}$ mice transferred with host-derived $CD25^{high}$ ($hCD25^{hi}$) cells (n = 3 per group) (* = $P < 0.02$ by *t*-test on day 41). Data are representative of 2 independent experiments. **C,** CD44 expression on CD4+CD25−FoxP3− cells in the spleens of B6.g7 mice and on host-derived CD4+CD25−FoxP3− cells in the spleens of K/BxN→B6.g7 chimeric mice killed 12 weeks after reconstitution. Values are the mean ± SEM from 4 K/BxN→B6.g7 mice and 3 B6.g7 mice. ** = $P < 0.005$ by *t*-test. Data are representative of 3 independent experiments with 4 mice per group. **D,** Expression of FR4 and CD73 on spleen cells in the CD4+CD25−FoxP3− population. Representative profiles from 1 of 3 mice are shown. Values are the mean ± SEM frequencies of CD73+FR4+ cells in all 3 groups (32 ± 4.6% among CD4+CD25−FoxP3− cells in normal B6.g7 mice, 62 ± 3.4% among host-derived CD4+CD25−FoxP3− cells in K/BxN→B6.g7 mice, 30.2 ± 2.8% among donor-derived CD4+CD25−FoxP3− cells in K/BxN→B6.g7 mice). $P < 0.0129$ for CD4+CD25−FoxP3− cells in normal B6.g7 mice versus host-derived CD4+CD25−FoxP3− cells in K/BxN→B6.g7 mice, by *t*-test; $P < 0.0021$ for host-derived CD4+CD25−FoxP3− cells in K/BxN→B6.g7 mice versus donor-derived CD4+CD25−FoxP3− cells in K/BxN→B6.g7 mice, by *t*-test. **E** and **F,** Mean fluorescence intensity (MFI) of CD73 (**E**) and FR4 (**F**) from host and donor-derived CD4+CD25−FoxP3− cells in the 2 groups of mice. Values are the mean ± SEM from 3 mice. ** = $P < 0.004$; *** = $P < 0.0009$ by *t*-test. Data are representative of 3 independent experiments. KBN = K/BxN (see Figure 1 for other definitions).

tuted mice (Figure 5A). Host-derived splenic CD4+ T cells were 15.2 ± 2.6% CD25+FoxP3+ compared to 6.7 ± 0.85% CD25+FoxP3+ among donor-derived CD4+ T cells ($P < 0.0059$); the latter value is similar to the Treg cell portion of CD4+ T cells in normal B6.g7 mice (8 ± 0.5%) (Figure 5A). The proportion of CD25+FoxP3+ cells in the donor-derived CD4+ T cells is not characteristic of CD4+ T cells expressing the transgenic KRN TCR. On the contrary, in K/BxN mice, Treg cells constitute 30% of the CD4+ T cell population (11). Similarly, in K/BxN→B6.g7 $Rag^{-/-}$ chimeras, the donor-derived CD4+ T cells included 26.5 ± 1.8% CD25+FoxP3+ T cells (Figure 5A).

To test their immunosuppressive capacity, we transferred host-derived $CD4+CD25^{high}$ T cells from K/BxN→B6.g7 mice (3 months after transfer of hematopoietic stem and progenitor cells) into K/BxN→B6.g7 $Rag^{-/-}$ mice 20 days after transfer of K/BxN hematopoietic stem and progenitor cells. Because FoxP3 is an intracellular protein and cannot be used as a marker for

sorting Treg cells, we used CD4+CD25^{high} T cells as a surrogate for CD4+CD25+FoxP3+ T cells (19,20). The K/BxN→B6.g7 Rag$^{-/-}$ mice were free of disease at the time of transfer. The mice were monitored for onset and progression of arthritis. We found that injected host-derived (CD45.2) CD4+CD25^{high} T cells delayed onset of disease when compared to control K/BxN→B6.g7 Rag$^{-/-}$ mice that received PBS (Figure 5B). However, by day 48 after T cell transfer, arthritis scores in both groups were comparable. At this time point, 55 ± 14.3% of the remaining host-derived CD45.2 cells were CD4+CD25+ cells (not shown).

Host-derived CD4+CD25−FoxP3− cells show a memory-like phenotype and express the suppression markers CD73 and FR4. As another potential source of suppressive host-derived CD4+ T cells, we assessed CD4+CD25−FoxP3− T cells for evidence of a regulatory phenotype. Radiation-resistant CD4+ T cells undergoing lymphopenia-induced proliferation in irradiated hosts acquire a memory-like phenotype, characterized by high expression of CD44 (21). These memory-like CD4+ T cells have suppressive effects on naive T cell proliferation (22). We found a higher percentage of host-derived CD4+CD25−FoxP3−CD44^{high} splenic T cells in K/BxN→B6.g7 mice compared to the percentage of this subset in B6.g7 mice (Figure 5C).

FR4 and CD73 are associated with regulatory function (23,24). Notably, the host-derived splenic CD4+CD25−FoxP3− cells in K/BxN→B6.g7 mice showed a significantly increased frequency of cells expressing both FR4 and CD73, compared to the donor-derived CD4+CD25−FoxP3− cells in K/BxN→B6.g7 mice ($P < 0.021$) or the CD4+CD25−FoxP3− cells in normal B6.g7 mice ($P < 0.0129$) (Figure 5D). The host-derived CD4+CD25− cells also showed higher expression (mean fluorescence intensity) of CD73 and FR4 than did the donor-derived CD4+CD25− T cells (Figures 5E and F). We tested the immunosuppressive capacity of these cells in adoptive transfer. Host-derived CD4+CD25−CD73+FR4+ cells from K/BxN→B6.g7 mice (3 months after transfer of hematopoietic stem and progenitor cells) also delayed disease onset when transferred into K/BxN→B6.g7 Rag$^{-/-}$ mice (Figure 5B). Thus, these host-derived FoxP3− cells could be contributing to protection against the manifestations of autoimmunity. These cells also persist (87 ± 9.19% of CD45.2 cells) in the recipient mice at day 48 (not shown), although their efficacy is overcome.

The phenotype of host-derived CD4+ T cells in the thymi of reconstituted mice. In K/BxN→B6.g7 mice, a high proportion (47.2 ± 2.36%) of host-derived CD4+ single-positive thymic cells were CD25+FoxP3+ (Figure 6A). Further, a higher percentage of host-derived CD4+ single-positive CD25− thymic cells were CD44^{high}, compared to donor-derived CD4+ single-positive CD25− thymic cells (Figure 6B), whereas CD4+ single-positive thymocytes typically are CD44^{low}. We also measured CD103, an $\alpha E\beta 7$ integrin previously shown to be ex-

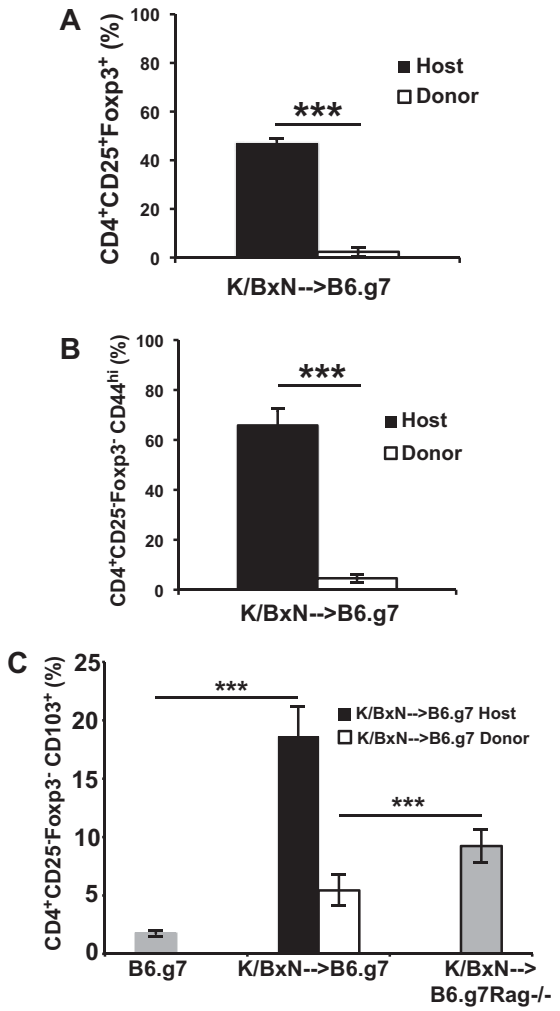

Figure 6. Thymocytes from K/BxN→B6.g7 mice have a higher frequency of host-derived Treg cells. **A,** Frequencies of CD4+CD25+FoxP3+ cells in the host- and donor-derived CD4+ single-positive thymocytes of the K/BxN→B6.g7 chimera. Values are the mean ± SEM from 3 animals in each group. *** = $P < 0.0001$ by *t*-test. Data are representative of 3 independent experiments. **B,** CD44 expression on host- or donor-derived CD4+CD25−FoxP3− cells in the thymi of the chimera killed 12 weeks after reconstitution. Values are the mean ± SEM from 3 animals in each group. *** = $P < 0.0005$ by *t*-test. Data are representative of 3 independent experiments. **C,** Frequency of CD103+ cells among host- and donor-derived CD4+CD25−FoxP3− cells in K/BxN→B6.g7 mice and in B6.g7 and K/BxN→B6.g7 Rag$^{-/-}$ mice. Values are the mean ± SEM from 5 animals in each group. *** = $P < 0.0003$ by *t*-test. See Figure 1 for definitions.

pressed on Treg cells (25) and on a unique subset of CD4+CD25− T cells that are suppressive in function (26). We found high CD103 expression on host-derived CD4+CD25−FoxP3− T cells in the thymi of K/BxN→B6.g7 mice compared to normal B6.g7 mice or to donor-derived CD4+CD25−FoxP3− T cells (Figure 6C). The host-derived and donor-derived splenic CD4+CD25−FoxP3− T cells expressed low levels of CD103 (data not shown). The expression of CD103 on the host-derived CD4+CD25−FoxP3− T cells in the thymus suggests a regulatory phenotype for these cells.

DISCUSSION

Transfer of hematopoietic stem and progenitor cells from K/BxN mice into B6.g7 $Rag^{-/-}$ mice results in disease similar to that in K/BxN mice. However, transfer of hematopoietic stem and progenitor cells into B6.g7 mice results in significant attenuation of arthritis. What regulates autoimmunity in the reconstituted mice? Arthritis in K/BxN mice is thought to be initiated by the extravasation of circulating anti-GPI–GPI immune complexes into joints, followed by complement-induced tissue destruction (27). Anti-GPI autoantibody titers in reconstituted K/BxN→B6.g7 chimeras are much lower than in K/BxN mice and K/BxN→B6.g7 $Rag^{-/-}$ chimeras. This is likely a key explanation for reduced arthritis in K/BxN→B6.g7 mice. This, in turn, implicates defect(s) in the T and/or B cell compartments of these mice. Data on chimerism in K/BxN→B6.g7 mice indicate that B cells and neutrophils are >98% donor (K/BxN) derived, and the fact that low levels of anti-GPI antibodies are produced demonstrates that the B cell compartment is competent to develop this specificity. In contrast, only ~10% of the peripheral CD4+ T cells in K/BxN→B6.g7 mice are donor derived, and the rest are host-derived CD4+ T cells that emerge despite irradiation, even at high (1,100-rad) doses (not shown).

The few donor-derived CD4+ T cells in the thymus and periphery of K/BxN→B6.g7 mice include a lower proportion of tetramer+V_β6+ cells than in K/BxN→B6.g7 $Rag^{-/-}$ mice and fewer thymic $V_\beta6^{intermediate}$ V_β8+ cells than in B6.g7 $Rag^{-/-}$ chimeras. This reduced level of donor-derived KRN TCR–expressing T cells may provide only limited amounts of help to GPI-specific B cells. In K/BxN mice, $V_\beta6^{intermediate}V_\beta$8+CD4+ T cells escape negative selection due to lower TCR affinity compared to V_β6+CD4+ T cells (13). The reduced proportion of donor-derived thymic $V_\beta6^{intermediate}V_\beta$8+CD4+ T cells in K/BxN→B6.g7 mice suggests increased negative selection of these thymocytes. Reduced frequency of circulating tetramer+CD4+ T cells in these mice also points to a process of negative selection. The mechanism of these phenomena is under investigation (also see below).

The surviving donor-derived CD4+ T cells are further restrained by immunosuppressive mechanisms. They are less activated in B6.g7 than in B6.g7 $Rag^{-/-}$ recipients, as reflected in a lower proportion that is $CD44^{high}$, and they have reduced levels of IFNγ and IL-17, 2 cytokines that are important for the development of arthritis in K/BxN mice (10,28). Key contributors to this suppression are likely the CD25+FoxP3+ cells that are enriched among the host-derived CD4+ T cells in the K/BxN→B6.g7 chimeras, persist even 3 months after transplant, and function to delay arthritis in adoptive transfer. Consistent with our results, residual, host-derived Treg cells allow survival of myeloablated B6 recipient mice following syngeneic BM transfer, whereas B6 $Rag^{-/-}$ recipients succumb to lethal syngeneic graft-versus-host disease (29). Interestingly, host-derived CD4+ T cells in K/BxN→B6.g7 mice do not expand to populate the lymphopenic CD4+ T cell compartment to achieve homeostatic proportions. The cause of this limitation needs to be investigated.

CD44, an activation and memory marker, is expressed at higher levels in the host-derived CD4+CD25−FoxP3− Teff cell population than in the donor-derived CD4+CD25−FoxP3− cells or in B6.g7 mice. This result also resembles observations in BM transplantation of syngeneic or Rag-deficient animals, where memory-like (CD44+) T cells are enriched in the host-derived CD4+ T cell compartment (6,21,22). Like conventional CD4+CD25+ Treg cells, a subset of memory-like $CD4+CD44^{high}$ T cells can also restrain activation and proliferation of naive T cells (23,24).

As a first step toward investigating immunosuppressive mechanisms of these cells in our model, we analyzed the CD4+CD25−FoxP3− cells for other markers of suppressive capacity, CD73 and FR4. CD73, a GPI-linked surface protein with ecto-5′-nucleotidase activity, mediates suppression by CD25+FoxP3+ T cells (23,30). CD39, an ecto-ATPDase that is also expressed by Treg cells and neutrophils, rapidly converts circulating ATP and ADP to 5′-AMP (31). Through its ecto-nucleotidase activity, CD73 converts 5′-AMP to adenosine (32). Adenosine mediates its immunoregulatory activities through various adenosine receptors expressed on T cells, B cells, neutrophils, and macrophages (33–35). In addition to Treg cells, a subset of memory-like CD4+ T cells expresses high levels of CD73 and is suppressive by producing adenosine (23). FR4 is one of the receptor subtypes for folic acid. FR4 is expressed at high levels on both natural and transforming growth

factor β–induced Treg cells. Host- and donor-derived conventional Treg cells (CD25+FoxP3+) in K/BxN→B6.g7 chimeras showed high expression of CD73 and FR4 (not shown). Strikingly, the conventional Teff cell or CD4+CD25−FoxP3− compartment also contains CD73+FR4+ cells, more so among host-derived cells, by percentages of positive cells and expression levels.

Martinez et al (36) recently showed that adoptive transfer of KRN T cells into lymphopenic TCR$\alpha^{-/-}$ I-A^{g7}+ hosts, but not I-A^{g7}+ wild-type mice, results in arthritis. They demonstrate that protection against arthritis is due to induction of anergy of KRN Teff cells via enhanced CD73 and FR4 expression. That study differed from ours in that we observed host-derived CD4+ T cells that exhibited a CD73+FR4+ phenotype. Adoptive transfer of these host-derived CD4+CD25−CD73+FR4+ cells from K/BxN→B6.g7 mice into K/BxN→B6.g7 Rag$^{-/-}$ mice also delayed onset of arthritis. To our knowledge, this is the first demonstration of high levels of CD73+FR4+ cells with possible regulatory properties, in the Teff cell compartment, persisting in mice after lethal irradiation.

Adoptive transfer of host-derived CD25^{high} cells or CD73+FR4+ T cells into K/BxN→B6.g7 Rag$^{-/-}$ mice leads only to delayed onset of disease and not to complete protection. This could be because additive or synergistic effects of these 2 regulatory populations are required for long-term control (both are present in K/BxN→B6.g7 mice).

The K/BxN→B6.g7 chimeras have a high frequency (65%) of host-derived thymic CD4+ T cells with a mature phenotype (CD44^{high}), which is uncharacteristic of CD4+ single-positive thymocytes. The latter are CD44^{low} and acquire the CD44^{high} phenotype in the periphery after encountering antigen. Thus, these CD44^{high} CD4+ T cells could have re-entered the thymus from the periphery. CD4+ T cells are capable of re-entering the thymus from the periphery under pathologic and lymphopenic conditions (22,37–39), and most of the re-entering cells are of the activated phenotype (39). The CD4+CD25−FoxP3− host-derived thymic CD4+ T cells in our model express CD103, an integrin that is induced at sites of inflammation and involved in the retention of T cells at these sites (40). CD103 expression also increases in response to IL-2 (41). Expression of CD103 on host-derived CD4+ T cells may mediate their retention in the thymi of the K/BxN→B6.g7 chimeras. Retention of circulating CD4+ T cells in the thymus has been shown to contribute to tolerance induction, specifically negative selection (37,39,42). Recirculating peripheral T cells also contribute to proper thymic organization and regeneration of the medullary thymic epithelium in an SCID mouse model (43). These cells may be responsible, at least in part, for the increased negative selection of KRN TCR–expressing CD4+ single-positive thymocytes in our model.

An alternative origin for host-derived CD4+ single-positive T cells in our model can be proposed, based on data from syngeneic BM transplant. Here, evidence suggested that the host-derived CD4+ T cells arose mainly from a transient wave of differentiation from radiation-resistant DN2 (CD4−CD8−CD25+CD44+) precursors within the thymus (6,44). The host-derived thymic CD4+ T cells of the K/BxN→B6.g7 chimera are also enriched for Treg cells. In a recent BM transplantation model, host-derived Treg cells required IL-2 for proliferation and IL-7 for survival (45). FoxP3 expression by the host-derived CD4+ single-positive cells in the K/BxN→B6.g7 chimera may result from increased thymic production of IL-2 due to robust negative selection (46).

In summary, persistent, host-derived CD4+ T cells with a high proportion of CD25+FoxP3+ cells and novel CD4+CD25−FoxP3−CD73+FR4+ cells are likely critical in protecting mice with autoimmune potential from full-blown disease. Recently, we found similar results using transfer of hematopoietic stem and progenitor cells carrying a transgenic, diabetogenic TCR into B6.g7 mice, indicating that the phenomena we observe are not unique to the KRN TCR and the arthritis model (Rajasekaran N, Mellins ED: unpublished observations). Our models will facilitate further study of the origin of host-derived CD4+ T cells and the mechanisms by which they mediate tolerance. Enrichment of these cell types is a potential therapeutic strategy in RA.

ACKNOWLEDGMENTS

We thank Drs. Diane Mathis and Christophe Benoist (Harvard Medical School, Boston, MA) for kindly providing the KRN mouse line, Dr. Luc Teyton (The Scripps Research Institute, La Jolla, CA) for kindly providing the MHC/GPI tetramers, and Dr. Andreas Hadjinicolaou (University of Cambridge, Cambridge, UK) for his assistance in assessment of arthritis in mice. We thank Jeanette Baker, Swati Acharya, and Suparna Dutt (Stanford University, Stanford, CA) for their useful discussions.

AUTHOR CONTRIBUTIONS

All authors were involved in drafting the article or revising it critically for important intellectual content, and all authors approved the final version to be published. Dr. Mellins had full access to all of the data in the study and takes responsibility for the integrity of the data and the accuracy of the data analysis.

Study conception and design. Rajasekaran, Mellins.
Acquisition of data. Rajasekaran, Wang, Truong, Macaubas, Beilhack.
Analysis and interpretation of data. Rajasekaran, Wang, Rinderknecht, Macaubas, Shizuru, Mellins.

REFERENCES

1. Cope AP. T cells in rheumatoid arthritis. Arthritis Res Ther 2008;10 Suppl 1:S1.
2. McInnes IB, O'Dell JR. State-of-the-art: rheumatoid arthritis. Ann Rheum Dis 2010;69:1898–906.
3. Mangialaio S, Ji H, Korganow AS, Kouskoff V, Benoist C, Mathis D. The arthritogenic T cell receptor and its ligand in a model of spontaneous arthritis. Arthritis Rheum 1999;42:2517–23.
4. Hugle T, van Laar JM. Stem cell transplantation for rheumatic autoimmune diseases. Arthritis Res Ther 2008;10:217.
5. De Kleer IM, Brinkman DM, Ferster A, Abinun M, Quartier P, Van Der Net J, et al. Autologous stem cell transplantation for refractory juvenile idiopathic arthritis: analysis of clinical effects, mortality, and transplant related morbidity. Ann Rheum Dis 2004;63:1318–26.
6. Bosco N, Swee LK, Benard A, Ceredig R, Rolink A. Autoreconstitution of the T-cell compartment by radioresistant hematopoietic cells following lethal irradiation and bone marrow transplantation. Exp Hematol 2010;38:222–32.e2.
7. Bayer AL, Jones M, Chirinos J, de Armas L, Schreiber TH, Malek TR, et al. Host $CD4^+CD25^+$ T cells can expand and comprise a major component of the Treg compartment after experimental HCT. Blood 2009;113:733–43.
8. Matsumoto I, Staub A, Benoist C, Mathis D. Arthritis provoked by linked T and B cell recognition of a glycolytic enzyme. Science 1999;286:1732–5.
9. Mandik-Nayak L, Allen PM. Initiation of an autoimmune response: insights from a transgenic model of rheumatoid arthritis. Immunol Res 2005;32:5–13.
10. Hickman-Brecks CL, Racz JL, Meyer DM, LaBranche TP, Allen PM. Th17 cells can provide B cell help in autoantibody induced arthritis. J Autoimmun 2011;36:65–75.
11. Monte K, Wilson C, Shih FF. Increased number and function of FoxP3 regulatory T cells during experimental arthritis. Arthritis Rheum 2008;58:3730–41.
12. Kang SM, Jang E, Paik DJ, Jang YJ, Youn J. $CD4^+CD25^+$ regulatory T cells selectively diminish systemic autoreactivity in arthritic K/BxN mice. Mol Cells 2008;25:64–9.
13. Kouskoff V, Korganow AS, Duchatelle V, Degott C, Benoist C, Mathis D. Organ-specific disease provoked by systemic autoimmunity. Cell 1996;87:811–22.
14. Beilhack GF, Scheffold YC, Weissman IL, Taylor C, Jerabek L, Burge MJ, et al. Purified allogeneic hematopoietic stem cell transplantation blocks diabetes pathogenesis in NOD mice. Diabetes 2003;52:59–68.
15. Stratmann T, Martin-Orozco N, Mallet-Designe V, Poirot L, McGavern D, Losyev G, et al. Susceptible MHC alleles, not background genes, select an autoimmune T cell reactivity. J Clin Invest 2003;112:902–14.
16. Solomon S, Rajasekaran N, Jeisy-Walder E, Snapper SB, Illges H. A crucial role for macrophages in the pathology of K/B × N serum-induced arthritis. Eur J Immunol 2005;35:3064–73.
17. Basu D, Horvath S, Matsumoto I, Fremont DH, Allen PM. Molecular basis for recognition of an arthritic peptide and a foreign epitope on distinct MHC molecules by a single TCR. J Immunol 2000;164:5788–96.
18. Nguyen LT, Jacobs J, Mathis D, Benoist C. Where FoxP3-dependent regulatory T cells impinge on the development of inflammatory arthritis. Arthritis Rheum 2007;56:509–20.
19. Suffia IJ, Reckling SK, Piccirillo CA, Goldszmid RS, Belkaid Y. Infected site-restricted Foxp3+ natural regulatory T cells are specific for microbial antigens. J Exp Med 2006;203:777–88.
20. Lewkowich IP, Herman NS, Schleifer KW, Dance MP, Chen BL, Dienger KM, et al. $CD4^+CD25^+$ T cells protect against experimentally induced asthma and alter pulmonary dendritic cell phenotype and function. J Exp Med 2005;202:1549–61.
21. Goldrath AW, Bogatzki LY, Bevan MJ. Naive T cells transiently acquire a memory-like phenotype during homeostasis-driven proliferation. J Exp Med 2000;192:557–64.
22. Bosco N, Agenes F, Rolink AG, Ceredig R. Peripheral T cell lymphopenia and concomitant enrichment in naturally arising regulatory T cells: the case of the pre-Tα gene-deleted mouse. J Immunol 2006;177:5014–23.
23. Kobie JJ, Shah PR, Yang L, Rebhahn JA, Fowell DJ, Mosmann TR. T regulatory and primed uncommitted CD4 T cells express CD73, which suppresses effector CD4 T cells by converting 5′-adenosine monophosphate to adenosine. J Immunol 2006;177:6780–6.
24. Yang L, Kobie JJ, Mosmann TR. CD73 and Ly-6A/E distinguish in vivo primed but uncommitted mouse CD4 T cells from type 1 or type 2 effector cells. J Immunol 2005;175:6458–64.
25. Banz A, Peixoto A, Pontoux C, Cordier C, Rocha B, Papiernik M. A unique subpopulation of $CD4^+$ regulatory T cells controls wasting disease, IL-10 secretion and T cell homeostasis. Eur J Immunol 2003;33:2419–28.
26. Lehmann J, Huehn J, de la Rosa M, Maszyna F, Kretschmer U, Krenn V, et al. Expression of the integrin $\alpha_E\beta_7$ identifies unique subsets of $CD25^+$ as well as $CD25^-$ regulatory T cells. Proc Natl Acad Sci U S A 2002;99:13031–6.
27. Wipke BT, Wang Z, Nagengast W, Reichert DE, Allen PM. Staging the initiation of autoantibody-induced arthritis: a critical role for immune complexes. J Immunol 2004;172:7694–702.
28. Jacobs JP, Wu HJ, Benoist C, Mathis D. IL-17-producing T cells can augment autoantibody-induced arthritis. Proc Natl Acad Sci U S A 2009;106:21789–94.
29. Benard A, Ceredig R, Rolink AG. Regulatory T cells control autoimmunity following syngeneic bone marrow transplantation. Eur J Immunol 2006;36:2324–35.
30. Deaglio S, Dwyer KM, Gao W, Friedman D, Usheva A, Erat A, et al. Adenosine generation catalyzed by CD39 and CD73 expressed on regulatory T cells mediates immune suppression. J Exp Med 2007;204:1257–65.
31. Eltzschig HK, Ibla JC, Furuta GT, Leonard MO, Jacobson KA, Enjyoji K, et al. Coordinated adenine nucleotide phosphohydrolysis and nucleoside signaling in posthypoxic endothelium: role of ectonucleotidases and adenosine A_{2B} receptors. J Exp Med 2003;198:783–96.
32. Zimmermann H. 5′-nucleotidase: molecular structure and functional aspects. Biochem J 1992;285:345–65.
33. Khoa ND, Montesinos MC, Reiss AB, Delano D, Awadallah N, Cronstein BN. Inflammatory cytokines regulate function and expression of adenosine A_{2A} receptors in human monocytic THP-1 cells. J Immunol 2001;167:4026–32.
34. McColl SR, St-Onge M, Dussault AA, Laflamme C, Bouchard L, Boulanger J, et al. Immunomodulatory impact of the A_{2A} adenosine receptor on the profile of chemokines produced by neutrophils. FASEB J 2006;20:187–9.
35. Panther E, Idzko M, Herouy Y, Rheinen H, Gebicke-Haerter PJ, Mrowietz U, et al. Expression and function of adenosine receptors in human dendritic cells. FASEB J 2001;15:1963–70.
36. Martinez RJ, Zhang N, Thomas SR, Nandiwada SL, Jenkins MK, Binstadt BA, et al. Arthritogenic self-reactive $CD4^+$ T cells acquire an $FR4^{hi}CD73^{hi}$ anergic state in the presence of $Foxp3^+$ regulatory T cells. J Immunol 2012;188:170–81.

37. Agus DB, Surh CD, Sprent J. Reentry of T cells to the adult thymus is restricted to activated T cells. J Exp Med 1991;173: 1039–46.
38. Michie SA, Kirkpatrick EA, Rouse RV. Rare peripheral T cells migrate to and persist in normal mouse thymus. J Exp Med 1988;168:1929–34.
39. Chau LA, Rohekar S, Wang JJ, Lian D, Chakrabarti S, Zhang L, et al. Thymic re-entry of mature activated T cells and increased negative selection in vascularized allograft recipients. Clin Exp Immunol 2002;127:43–52.
40. Suffia I, Reckling SK, Salay G, Belkaid Y. A role for CD103 in the retention of $CD4^+CD25^+$ T_{reg} and control of Leishmania major infection. J Immunol 2005;174:5444–55.
41. Sharma R, Sung SS, Abaya CE, Ju AC, Fu SM, Ju ST. IL-2 regulates CD103 expression on $CD4^+$ T cells in Scurfy mice that display both CD103-dependent and independent inflammation. J Immunol 2009;183:1065–73.
42. Irla M, Hugues S, Gill J, Nitta T, Hikosaka Y, Williams IR, et al. Autoantigen-specific interactions with $CD4^+$ thymocytes control mature medullary thymic epithelial cell cellularity. Immunity 2008;29:451–63.
43. Surh CD, Ernst B, Sprent J. Growth of epithelial cells in the thymic medulla is under the control of mature T cells. J Exp Med 1992;176:611–6.
44. Kadish JL, Basch RS. Thymic regeneration after lethal irradiation evidence for an intra-thymic radioresistant T cell precursor. J Immunol 1975;114:452–8.
45. Bayer AL, Chirinos J, Cabello C, Yang J, Matsutani T, Malek TR, et al. Expansion of a restricted residual host T_{reg}-cell repertoire is dependent on IL-2 following experimental autologous hematopoietic stem transplantation. Eur J Immunol 2011;41:3467–78.
46. Bassiri H, Carding SR. A requirement for IL-2/IL-2 receptor signaling in intrathymic negative selection. J Immunol 2001;166: 5945–54.

DOI 10.1002/art.37793

Clinical Image: Raccoon sign

The patient, a 72-year-old man, presented with an 18-month history of fatigue, dizziness, and exercise dyspnea. On physical examination, periorbital ecchymosis ("raccoon sign" or "panda eyes") and postural hypotension without increased heart rate were noted. Proteinuria was measured by 24-hour urine collection (protein level 2.6 grams), and serum monoclonal paraprotein (κ light chain) was detected. An echocardiogram showed thickening of the ventricular walls and diastolic dysfunction. A bone marrow biopsy specimen contained 46% plasma cells. Soon after diagnosis, he developed pneumonia and died 20 days later. Skin involvement is one of the most characteristic manifestations of primary amyloidosis (AL amyloidosis). Usually nonpruritic lesions consist of slightly raised, waxy papules or plaques clustered in the folds of the axillae, anal, or inguinal regions. Although it occurs only in about one-fifth of patients with AL amyloidosis, periorbital ecchymoses are considered pathognomonic of this disease. These typical lesions are due to intracutaneous hemorrhage, resulting from amyloid infiltration and weakening blood-vessel walls.

Carlos G. G. de Moura, MD, PhD
Constança M. S. Cruz, MD, PhD
Sérgio P. de Souza, MD
Hospital Santo Antônio
Salvador, Brazil